Self-Similar Shrinkers in $\mathbb{R}^3$

Tobias Kohn

Diploma Thesis
ETH Zürich, Department of Mathematics

Advisor Prof Tom Ilmanen

January 2008

Contents

1 Introduction

Variations A geodesic is known to be locally the shortest path between two points p and q on a Riemannian manifold. If we introduce the length functional $L[\gamma]$ that assigns to each curve γ its length according to the Riemannian metric, then a geodesic γ_0 becomes the curve which locally minimizes the length functional $L[\gamma]$. That is if we slightly alter γ_0, $L[\gamma]$ does not decrease.

In finite-dimensional calculus a necessary condition for x_0 to be a minimum of a function $f(x)$ is that the derivative vanishes $\frac{d}{dx}f(x_0) = 0$. Since the variable of $L[\gamma]$ is a function itself, γ is infinite-dimensional and it is therefore not clear what $\frac{d}{d\gamma}L[\gamma]$ should mean. To overcome this obstacle we introduce a vector field X along γ_0 and set $\gamma_s(x) := \gamma_0(x) + s \cdot X(x)$. Using such vector fields X as basis we say: The functional $L[\gamma]$ has an extremum at $\gamma = \gamma_0$ if for every vector field X:

$$\left.\frac{d}{ds}\right|_{s=0} L[\gamma_s] = 0.$$

This is called the *first variation* of L and sometimes denoted as δL or $\delta^1 L$. A curve γ_0 with $\frac{d}{ds}\big|_{s=0} L[\gamma_s] = 0$ is also called a *stationary point* for $L[\gamma]$. Accordingly one can also define the *second variation* by

$$\delta^2 L = \left.\frac{d^2}{ds^2}\right|_{s=0} L[\gamma_s].$$

The area and mean curvature flow Analogous to the length functional $L[\gamma]$ we can define an area functional $A[S]$ for a surface S. Stationary points for $A[S]$ are then called *minimal surfaces*. So a minimal surface is indeed a surface that locally minimizes the area. It turns out that the condition $\delta A[S] = 0$ is equivalent to the mean curvate vector $\vec{H}$ being zero for every point x on S.

In physics the idea of geodesics and minimal surfaces has various applications. For example Newton's axiom stating that any object moves along geodesics unless forced otherwise ($\ddot{x} = 0$). Soap films also tend to form minimal surfaces (with certain constraints as for example the included volume that keeps a soap bubble from collapsing). If we start off with any soap film it will change shape until it has reached a stationary point for the area functional under the given constraints.

The tendency of curves and surfaces to change shape to minimize the length or

area functional can be modelled by *mean curvature flow* (MCF):

$$\frac{\partial}{\partial t}x = \vec{H}(x).$$

It says that each point of the surface moves according to the mean curvature at

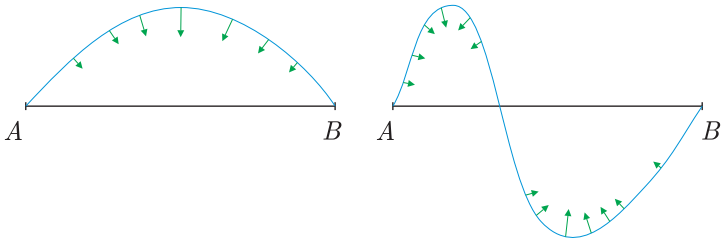

Figure 1: *Two examples of curves with mean curvature vectors. Under mean curvature flow the curves with fixed endpoints move towards a geodesic.*

this point. Because of the first variation formula

$$\delta A[N] = -\int_N \langle X, \vec{H}\rangle d\mathcal{H}^2,$$

it is obvious that mean curvature flow (for which we have $X = \vec{H}$) decreases the area of any surface except of course for minimal surfaces.

If a surface is compact and no other constraints are given, mean curvature flow will cause it to collapse and disappear within finite time. This is not surprising: a singular surface consisting of a point alone has always less area than any other surface which has positive area.

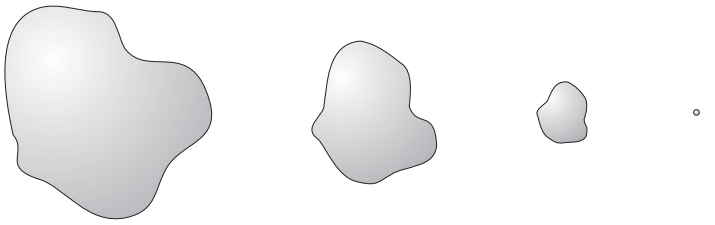

Figure 2: *Compact surfaces that evolve under mean curvature flow disappear in finite time.*

During the process of minimizing the area functional a surface can build singularities and change its topology. It is this singularity building process we are interested in.

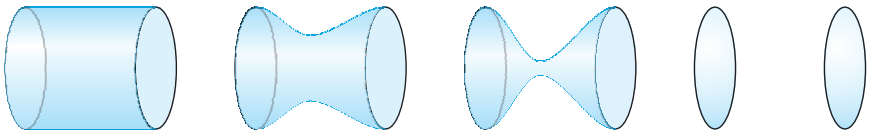

Figure 3: *A soap film changing its topology from a simply connected cylinder to that of two disjoint discs.*

Singularities When a compact convex surface shrinks to a point it becomes more and more spherical and by the time it vanishes it would have become a sphere (see figure 2). To observe this more easily we could impose a volume constraint on the interior of the surface. Then the surface will not shrink at all but change shape into a sphere, which is known to be the minimizer for the area under a given volume.

The convergence of convex compact surfaces to a spherical point leads to another question regarding singularities: assume a surface N does develop another singularity p before the surface has shrunk down to a point (if it does shrink at all). Then does the surface at p also converge to a regular or special shape like the sphere in the case of convex surfaces?

Under certain circumstances the answer is definitely "yes". The limiting surfaces found at such singularities are self-similar shrinking surfaces. Self-similar means that they do change size but not shape under mean curvature flow. It is the aim of this paper to investigate such self-shrinking surfaces.

Acknowledgements

The author is deeply indebted to Tom Ilmanen. He has provided exceptional mentoring and spent many hours explaining details not yet understood by the author.

2 Preliminaries

In this section we will establish the notation used throughout this paper. We will also prove some lemmata used later. The reader might skip this section and come back as needed.

Note that we will restrict ourselves completely to the case of surfaces inside $\mathbb{R}^3$. This simplifies notation and some calculations.

Some of the used symbols are:

$\langle \cdot, \cdot \rangle$	Euclidean scalar product.
τ_1, τ_2	Orthonormal basis of $T_x N$.
ν	Unit normal to $T_x N$.
$X^\top$, $X^\perp$	Tangential and normal projection of X to $T_x N$.
H, $\vec{H}$	Mean curvature and mean curvature vector.
$\operatorname{div}_N X$	Divergence of X with respect to N.
II	Second fundamental form.
$\mathcal{H}^n$	n-dimensional Hausdorff measure.

2.1 Notation

Vectors and derivatives Elements of $\mathbb{R}^3$ and vectors will be written without a special marker. Only the mean curvature vector $\vec{H}$ will be distinguished from its scalar counterpart H. The euclidean scalar product will be written as $\langle \cdot, \cdot \rangle$, whereas the dot $\cdot$ is never used for a scalar product.

For a surface $N \subset \mathbb{R}^3$ let $\tau_1(x), \tau_2(x)$ be an orthonormal basis for the tangent space $T_x N$ and $\nu(x)$ the unit normal vector. For simplification we will suppress the dependance on x and just write τ_1, τ_2 and ν, respectively.

Let $X : \mathbb{R}^3 \to \mathbb{R}^3$ be a vector field. Then we can write the derivative of X in the direction of τ as:

$$D_\tau X = DX \cdot \tau,$$

where $(DX)_i^j = (\partial_i X^j)$ is the jacobian matrix of X. The divergence of X with respect to N is

$$\operatorname{div}_N X := \langle D_{\tau_1} X, \tau_1 \rangle + \langle D_{\tau_2} X, \tau_2 \rangle.$$

Analogous we have for a function $f : \mathbb{R}^3 \to \mathbb{R}$ the derivative in direction of τ:

$$D_\tau f(x) = \langle Df, \tau \rangle,$$

where $(Df)_i = \partial_i f$ is the gradient of f. Similar to the divergence it is

$$D_N f := D_{\tau_1} f \cdot \tau_1 + D_{\tau_2} f \cdot \tau_2.$$

We will also denote the intrinsic derivative of a function $u : N \to \mathbb{R}$ by $D_N u$.

For any vector field X, the tangential part of X is denoted by $X^\top$ and $X^\perp$ is the part perpendicular to N, i. e.:

$$X^\top = \langle X, \tau_1 \rangle \tau_1 + \langle X, \tau_2 \rangle \tau_2, \qquad X^\perp = \langle X, \nu \rangle \nu.$$

Metric and curvature As usual the metric is denoted by g_{ij} and its inverse by g^{ij}. The second fundamental form will be denoted by II. Note that for an embedding $F : M \to \mathbb{R}^3$ of M into $\mathbb{R}^3$ the metric is

$$g_{ij} = \langle \partial_i F, \partial_j F \rangle.$$

The second fundamental form then is

$$\mathrm{II}_{ij} = \langle \partial_i \nu, \partial_j F \rangle = -\langle \nu, \partial_i \partial_j F \rangle.$$

The equivalence of these two expressions for II follows from the fact that $\langle \nu, \partial_i F \rangle = 0$ for all i.

Mean curvature plays a crucial role in our paper. It is denoted by H, whereas $\vec{H}$ will denote the mean curvature vector. We have

$$H := -\operatorname{div}_N \nu = -g^{ij} \mathrm{II}_{ij}, \qquad \vec{H} = H\nu.$$

Note that there is no canonical form for H. Some treatments define mean curvature with an opposite sign such that $\vec{H} = -H\nu$. Others use $H = \frac{1}{n} \operatorname{div}_N \nu$. This causes sometimes slight differences between our result and that of other papers.

Integration Most of the integrals will be with respect to the euclidean area. For the later we use the Hausdorff measure $\mathcal{H}^n$. However the results do not depend on special properties of the Hausdorff measure so the reader might just read it as euclidean length ($\mathcal{H}^1$) or area ($\mathcal{H}^2$) respectively.

The exact definition of $\mathcal{H}^n$ can be found in any book about Geometric measure theory.

2.2 Some lemmata

This section contains some lemmata that are rather techincal. As mentioned before the reader might skip this section and come back as needed.

Lemma 1 *For a function $f : \mathbb{R}^3 \to \mathbb{R}$ and a vector field $X : \mathbb{R}^3 \to \mathbb{R}^3$ we have:*

$$\operatorname{div}_N(f \cdot X) = f \cdot \operatorname{div}_N X + \langle X, (Df)^\top \rangle.$$

In the special case of $X = \nu$ we get

$$\operatorname{div}_N(f \cdot \nu) = f \cdot \operatorname{div}_N \nu.$$

Proof

$$\begin{aligned}
\operatorname{div}_N(f \cdot X) &= D_{\tau_1}(f \cdot X) \cdot \tau_1 + D_{\tau_2}(f \cdot X) \cdot \tau_2 \\
&= f \cdot \langle D_{\tau_1} X, \tau_1 \rangle + D_{\tau_1} f \langle X, \tau_1 \rangle + f \cdot \langle D_{\tau_2} X, \tau_2 \rangle + D_{\tau_2} f \langle X, \tau_2 \rangle \\
&= f \cdot \operatorname{div}_N X + \langle X, D_{\tau_1} f \cdot \tau_1 + D_{\tau_2} f \cdot \tau_2 \rangle \\
&= f \cdot \operatorname{div}_N X + \langle X, (Df)^\top \rangle
\end{aligned}$$

For $X = \nu$ the second term obviously vanishes: $\langle \nu, (Df)^\top \rangle = 0$. □

Lemma 2 *Let $X : N \to \mathbb{R}^3$ be a vector field on a submanifold $N \subset \mathbb{R}^3$ with compact support (i. e. $X \equiv 0$ on ∂N if $\partial N \neq \emptyset$). Then*

$$\int_N \operatorname{div}_N X = -\int_N \langle \vec{H}, X \rangle,$$

where $\vec{H}$ is the mean curvature vector of N.

Proof Split the vector field X into the tangential and the normal component $X = X^\top + X^\perp$. Then $X^\perp = \langle X, \nu \rangle \nu$ and with Lemma 1 for $f = \langle X, \nu \rangle$ we obtain:

$$\begin{aligned}
\operatorname{div}_N X^\perp &= \operatorname{div}_N(\langle X, \nu \rangle \nu) \\
&= \langle \nu, X \rangle \cdot \operatorname{div}_N \nu \\
&= \langle \operatorname{div}_N \nu \cdot \nu, X \rangle \\
&= -\langle \vec{H}, X \rangle.
\end{aligned}$$

The tangential component $X^\top$ can locally be regarded as a vector field $\tilde{X} : \mathbb{R}^2 \to \mathbb{R}^2$. Therefore we can apply the divergence theorem in two dimensions:

$$\int_N \operatorname{div}_N X^\top = \int_{\partial N} \langle X^\top, \vec{n} \rangle,$$

where $\vec{n}$ is the unit normal along ∂M inside $T_x N$. But because X has compact support the right hand side is zero and therefore:

$$\int_N \operatorname{div}_N X = \int_N \operatorname{div}_N X^\top + \operatorname{div}_N X^\perp = 0 - \int_N \langle \vec{H}, X \rangle.$$

□

Lemma 3 *Let $A, B \in \mathbb{R}^{2\times 2}$ be two matrices. Then*

$$\det(I + At + Bt^2) = 1 + t \cdot \operatorname{tr} A + t^2(\det A + \operatorname{tr} B) + \mathcal{O}(t^3),$$

where I is the unity matrix $I_{ij} = \delta_{ij}$.

Proof

$$\begin{aligned} \det(I + At + Bt^2) &= \left(1 + a_{11}t + b_{11}t^2\right)\left(1 + a_{22}t + b_{22}t^2\right) \\ &\quad - \left(a_{12}t + b_{12}t^2\right)\left(a_{21}t + b_{21}t^2\right) \\ &= 1 + t(a_{11} + a_{22}) + t^2(b_{11} + b_{22} + a_{11}a_{22} - a_{12}a_{21}) \\ &= 1 + \operatorname{tr} A + t^2(\det A + \operatorname{tr} B). \end{aligned}$$

□

Lemma 4 *For the second fundamental form* II *of a surface N inside $\mathbb{R}^3$ it is:*

$$2\det(\mathrm{II}) = H^2 - |\,\mathrm{II}\,|^2,$$

where $|\,\mathrm{II}\,|^2 = \mathrm{II}^i_j\,\mathrm{II}^j_i$.

Proof Set

$$\mathrm{II} = \begin{bmatrix} a_{11} & a_{12} \\ a_{21} & a_{22} \end{bmatrix}.$$

Then

$$\begin{aligned} |\,\mathrm{II}\,|^2 &= a_{11}a_{11} + a_{12}a_{21} + a_{21}a_{12} + a_{22}a_{22} \\ &= (a_{11} + a_{22})^2 - 2a_{11}a_{22} + 2a_{12}a_{21} \\ &= (\operatorname{tr}(\mathrm{II}))^2 - 2\det(\mathrm{II}). \end{aligned}$$

□

3 Selfsimilar solutions to mean curvature flow

3.1 Mean curvature flow

A surface can be considered as a 2-manifold M with a smooth embedding $F : M \to \mathbb{R}^3$. To have the surface evolve with time we extend F to depend on a time variable t and get:

$$\begin{aligned} F : M \times I &\to \mathbb{R}^3 \\ (p,t) &\mapsto x \end{aligned}$$

This leads to a family of surfaces $\{N_t\}_t \subset \mathbb{R}^3$. For convenience of notation we will mostly drop the embedding F and directly consider the surfaces N_t.

A family of smoothly embedded surfaces $\{N_t\}_t$ moves by *mean curvature flow* if for all $x \in N_t$:

$$\frac{\partial x}{\partial t} = \vec{H}(x). \tag{MCF}$$

It says that the velocity of any point $x \in N_t$ is given by its mean curvature.

The actual parametrization of the surfaces N_t is of no interest to us. So we ignore any tangential motions within N_t and assume that the N_t's are parametrized such that the velocity $\frac{\partial x}{\partial t}$ is indeed perpendicular to $T_x N_t$.

Minimal surfaces Because minimal surfaces have zero mean curvature everywhere they do not evolve under mean curvature flow at all. There is a wide variety of known minimal surfaces today. Two of the best-known are the plane and the catenoid. Another example that will be of interest to us is the *Scherk surface* or *Scherk tower* (There are other minimal surfaces also called *Scherk surface* but we will always refer to this one). The special thing about this surface is that it provides a possiblity to desingularize the intersection of two surfaces.

If for instance two planes intersect the result is not a submanifold of $\mathbb{R}^3$ anymore – it is singular along the intersection line. To prevent this singularity one could bend the two planes so that they do not intersect anymore, in a way similar to hyperbolas. There are two possible ways of doing so and by combining them one gets the Scherk tower.

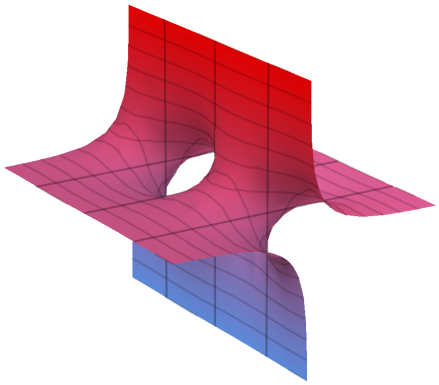

Figure 4: *A piece of the Scherk tower.*

An implicit formula for the Scherk tower is

$$\sinh(x) \cdot \sinh(z) = \sin(y),$$

where x, y and z denote the usual coordinates of $\mathbb{R}^3$. It is an easy exercise to verify that mean curvature for this surface is zero everywhere.

Selfsimilar surfaces Another import class of solution to the mean curvature flow are self-similar surfaces. In contrast to minimal surfaces which are stationary self-similar surfaces are allowed to move (translate), shrink or expand. However besides shrinking or expanding they do not change shape.

An example of a self-shrinker is the sphere. The sphere is a most regular figure but under mean curvature flow it is not stationary. It shrinks down to a single point. But even though the sphere shrinks it stays a sphere for all the time it is defined (before it becomes a singularity) und thus it is a fine example of a self-shrinker. We will discuss self-similar surfaces in greater detail below.

3.2 Singularities

Apart from minimal and self-similar surfaces any smoothly embedded surface in $\mathbb{R}^3$ can be evolved under mean curvature flow. However a common surface is likely to develop singularities in finite time and thereby cease to be a regular embedded surface.

Convex surfaces If a surface is compact and convex it will not build any singularities before it shrinks down to a point. By convex we mean that the prinicipal curvatures, that is the eigenvalues of the second fundamental form, all have the same sign for every point. The actual sign depends on the choice of a unit normal field. This result is due to Huisken.

Huisken showed even more. Such a convex compact surface will become more and more spherical as it shrinks down to a point. Because it does not make much sense to speak about a spherical singularity we have to normalize the surfaces N_t in order to state an exact result.

So let $\Phi_t : \mathbb{R}^3 \to \mathbb{R}^3$ be a homothety (i. e. there is a $\lambda_t \in \mathbb{R}_{>0}$ such that for every point $x \in \mathbb{R}^3$ it is $\Phi_t(x) = \lambda_t \cdot x$). Then normalize the surfaces N_t such that their area remains constant: $\tilde{N}_t = \Phi_t \cdot N_t$ with

$$\int_{\tilde{N}_t} d\mathcal{H}^2 = \int_{N_0} d\mathcal{H}^2,$$

where N_0 shall denote the initial surface. Let furthermore T be the time where N_t becomes singular for the first time. Then for any convex compact initial surface N_0 the normalized surfaces $\tilde{N}_t$ will converge to a sphere with the same area as N_0 as $t \to T$.

After introducing a new time variable $\tilde{t}$ such that the surfaces $\tilde{N}_{\tilde{t}}$ are defined for all $0 \leq \tilde{t} < \infty$, Huisken's exact result is as follows:

Theorem 5 (Huisken, 1984) *Let $n \geq 2$ and assume that M_0 is uniformly convex, i. e., the eigenvalues of its second fundamental form are stricly positive everywhere. Then the evolution equation (MCF) has a smooth solution on a finite time interval $0 \leq t < T$, and the M_t's converge to a single point O as $t \to T$. The normalized equation has a solution $\tilde{M}_{\tilde{t}}$ for all time $0 \leq \tilde{t} < \infty$. The surfaces $\tilde{M}_{\tilde{t}}$ are homothetic expansions of the M_t's, and if we choose O as the origin of $\mathbb{R}^{n+1}$, then the surfaces $\tilde{M}_{\tilde{t}}$ converge to a sphere of area $|M_0|$ in the C^∞-topology as $\tilde{t} \to \infty$.*

Limiting surfaces for singularities According to Huisken's result any convex compact surface shrinks down to a point and converges thereby to a sphere. When the surface is not convex we cannot expect it to become spherical in the limit as $t \to T$ anymore, even if it shrinks down to a point. It is likely to develop another singularity before T and change its topology.

Since convex surfaces are converging to the sphere we might ask if other "singularitiy points" still converge to special surfaces. A few years after his first result Huisken has also given the answer to this question.

Let p be a singularity point of N_t at the time $t = T$. Assume furthermore that the second fundamental form does not grow too fast (will be made more precise below). Then a neighborhood of p will converge to a self-shrinking surface as $t \to T$.

In other words self-shrinking surfaces are a means to describe the singularities that evolve under mean curvature flow. Understanding these self-shrinkers will lead to a better understanding of the singularities and give a means to evolve a surface past the time of its first singularity.

Let us state Huisken's result more precisely. Assume that there is an upper bound for the blow-up rate of the second fundamental form of the form

$$\max_{N_t} |\,\mathrm{II}\,|^2 \leq \frac{C_0}{2(T-t)} \tag{1}$$

for a constant C_0 and T being the time where the first singularity occurs. As before normalize the surfaces N_t and time t:

$$\tilde{N}_{\tilde{t}} = \frac{1}{\sqrt{2(T-t)}} N_t, \qquad \tilde{t} = \log \frac{1}{\sqrt{2(T-t)}}.$$

Then we get the following theorem:

Theorem 6 (Huisken, 1990) *Suppose (1) is satisfied. Then for each sequence $\tilde{t}_j \to \infty$ there is a subsequence $\tilde{t}_{jk}$ such that $\tilde{N}_{\tilde{t}_{jk}}$ converges smoothly to an immersed nonempty limiting surface $\tilde{M}_\infty$.*

Each such limiting surface $\tilde{M}_\infty$ satisfies the equation

$$H = -\frac{\langle x, \nu \rangle}{2},$$

where x ist the position vector, H is the mean curvature and ν is the unit normal such that the mean curvature vector is given by $\vec{H} = H\nu$.

3.3 Self-Shrinkers

A self-similar shrinker is a surface that shrinks under (MCF) homothetically. because of theorem 6 such self-shrinkers play a role as limiting surfaces for

singularities. In this section we deduce a special equation that holds for any self-shrinker.

For convenience assume that the time at which the surface N_t becomes singular is $T = 0$. Then the surface does exist for $t < 0$ only. We furthermore impose the ansatz

$$N_t = \lambda(t) \cdot N_1,$$

where $\lambda : \mathbb{R}_{\leq 0} \to \mathbb{R}_{\geq 0}$ ist the homothety factor and N_1 is the surface at time $t = -1$. Clearly we have $\lambda(-1) = 1$ and $\lambda(0) = 0$ with this setting.

Accoding to (MCF) $H(x)$ gives the velocity of any point $x \in N_t$. The smaller the surface the larger $H(x)$, in fact we have

$$H(\lambda x) = \frac{1}{\lambda} H(x). \tag{2}$$

Thus we expect the shrinking process to accelerate as $t \to 0$. In other words $\lambda(t)$ is supposed to have a graph similar to the one in figure 5.

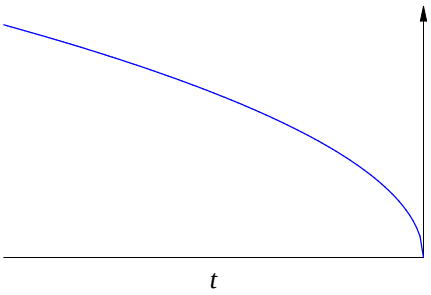

Figure 5: *The shrinking process of a surface N is supposed to accelerate as $t \to 0$.*

To see (2) let $x = F(u, v)$ be the embedding of M into $\mathbb{R}^3$. Then the homothetically expanded surface has the embedding $\tilde{F} = \lambda \cdot F$. Of course the metric and second fundamental form change accordingly:

$$\tilde{g}_{ij} = \langle \partial_i \tilde{F}, \partial_j \tilde{F} \rangle = \lambda^2 g_{ij}, \qquad \tilde{\mathrm{II}}_{ij} = -\nu \partial_i \partial_j \tilde{F} = -\lambda \nu \partial_i \partial_j F = \lambda \, \mathrm{II}_{ij} \, .$$

For H we then get

$$\tilde{H} = \tilde{g}^{ij} \, \mathrm{II}_{ij} = \frac{1}{\lambda^2} g^{ij} \cdot \lambda \, \mathrm{II}_{ij} = \frac{1}{\lambda} H.$$

Now put the ansatz $N_t = \lambda(t) \cdot N_1$ into (MCF):

$$\frac{\partial}{\partial t}(\lambda(t) \cdot x) = \frac{\vec{H}}{\lambda(t)}$$

which leads to

$$\frac{d\lambda}{dt} \cdot \lambda \cdot x = \vec{H}. \tag{3}$$

Because $\vec{H}$ and x do not depend on t we get the ODE:

$$\frac{d\lambda}{dt} \cdot \lambda = C$$

and thus

$$\lambda(t) = \sqrt{C \cdot t}.$$

Through the conditions $\lambda(0) = 0$ and $\lambda(-1) = 1$ we finally get

$$\lambda(t) = \sqrt{-t}.$$

If we put this back into (3) and with $\lambda' \cdot \lambda = -\frac{1}{2}$ we obtain the self-shrinker equation:

$$-\frac{1}{2}x = \vec{H}$$

or

$$H + \frac{\langle x, \nu \rangle}{2} = 0. \tag{SS}$$

Any self-shrinking surface N_t is a solution for (SS) for $t = -1$. The equation (SS) does not only impose constraints on the shape but also on the specific size of a surface. For example we will see that the sphere is only a solution to (SS) if it has radius $R = 2$. This does not mean that a larger or smaller sphere will not shrink homothetically but any sphere that is supposed to shrink to a singularity at $t = 0$ must have radius $R = 2$ at time $t = -1$.

There are only a few known solutions to (SS). These include the sphere, the cylinder, the plane and a doughnut found by Angenent. However there are numerical indications of further solutions.

In general minimal surfaces are not a solution to (SS). Because of $H = 0$ for all $x \in N$ we have $\langle x, \nu \rangle = 0$ which is only true for cones and of which only the plane is a smoothly embedded minimal surface.

Sphere and cylinder The mean curvature of the sphere S^2 is well known to be $H = \frac{-2}{R}$, where R is the radius. It is also obvious that $x = R\nu$ for all $x \in S^2$ and therefore (SS) becomes:

$$-\frac{2}{R} + \frac{R}{2} = 0.$$

So the sphere is clearly a solution to (SS) with the radius at $t = -1$ being $R = 2$.

Analogous the mean curvature of a cylinder C with radius R is $H = \frac{-1}{R}$. On the other hand $\langle x, \nu \rangle = R$ for all $x \in C$. So (SS) becomes:

$$-\frac{1}{R} + \frac{R}{2} = 0,$$

which yields $R = \sqrt{2}$.

Angenent's doughnut To prove that the torus found by Angenent is a self-shrinker is beyond the scope of this paper. However we state the main result and give a sketch of the proof.

Theorem 7 (Angenent, 1989) *For $n \geq 2$ there exist embeddings $F_n : S^1 \times S^{n-1} \to \mathbb{R}^{n+1}$ for which $F_n(p,t) = \sqrt{-t} \cdot F_n(p)$ is a solution of the mean curvature flow (MCF).*

The proof makes strong use of the rotation symmetry of the torus. In fact Angenents method could be used to find any self-shrinker obtained by rotating a curve $\gamma \subset \mathbb{R}^2$.

Angenent shows that the surface N obtained through rotation of the curve γ is a self-shrinker iff the curve γ is a geodesic for a special metric bestowed upon $\mathbb{R}^2$. The problem of finding a self-similar torus is thus reduced to finding a geodesic on a two-manifold. The existence of a symmetric closed curve γ is then proven with the theory of differential equations.

We will come back to Angenent's doughnut later on.

4 First and second variation

The problem with the self-shrinker equation (SS) is that it must hold for every point $x \in N$. For a surface N that is not as highly symmetric as are the sphere or the cylinder it can become quite difficult and cumbersome to check (SS) for all $x \in N$. Thus it would be handy to have a global equation or characterization for self-shrinkers N, equivalent to (SS). Such a characterization is provided by a functional $J[N]$ which we will derive in this section.

Minimal surfaces are stationary for the area functional $A[N]$, i. e. $\delta A[N] = 0$ for any minimal surface N. On the other hand N also satisfies $H = 0$ for every point $x \in N$. So the local equation $H = 0$ corresponds to the global equation $\delta A[N] = 0$.

Although self-shrinkers are not stationary for $A[N]$ it is possible to find another functional $J[N]$ for which self-shrinkers are stationary. Hence $\delta J[N] = 0$ will be equivalent to (SS). In order to find $J[N]$ we impose the ansatz

$$J[N] = \int_N f(x) d\mathcal{H}^2$$

for a function $f : \mathbb{R}^3 \to \mathbb{R}$, and try to determine $f(x)$. In this we will mainly follow Ilmanen's approach.

However the idea of the functional $J[N]$ is due to Huisken. He discovered that for the *backward heat kernel*

$$\rho(x,t) = \frac{1}{(-4\pi t)^{n/2}} \cdot \exp\left(\frac{|x|^2}{4t}\right), \qquad t < 0$$

equation (MCF) implies the following monotonicity formula.

Theorem 8 (Huisken, 1990) *If a surface N_t satisfies (MCF) for $t < 0$ then we have the monotonicity formula*

$$\frac{d}{dt}\int_{N_t} \rho(x,t) d\mu_t = -\int_{N_t} \rho(x,t) \left|\vec{H} - \frac{1}{2t}\vec{F}^{\perp}\right| d\mu_t.$$

4.1 The Jacobian

To calculate the first and second variation we will use the jacobian of some diffeomorphisms ψ_t. The aim of this section is to prove the following formula

for the jacobian:

$$J\psi_t = 1 + t\,\mathrm{div}_N\, X + \frac{t^2}{2}\left(\mathrm{div}_N\, Z + \left|(D_{\tau_1}X)^\perp\right|^2 + \left|(D_{\tau_2}X)^\perp\right|^2 + 2\Lambda\right).$$

These calculations are inspired by the first and second variation formulae that can be found in Simon's treatise [13].

Let U be an open subset of $\mathbb{R}^3$ and let $\{\phi_t\}_t$ be a family of diffeomorphisms $U \to U$ such that $\phi_0(x) = x$. Let X and Z denote the initial velocity and acceleration vectors for ϕ_t:

$$X = \left.\frac{\partial \phi_t(x)}{\partial t}\right|_{t=0}, \qquad Z = \left.\frac{\partial^2 \phi_t(x)}{\partial t^2}\right|_{t=0}.$$

Then

$$\phi_t(x) = x + tX + \frac{t^2}{2}Z + \mathcal{O}(t^3).$$

Let ψ be the restriction of ϕ to N:

$$\psi_t := \left.\phi_t\right|_N.$$

We want to calculate the jacobian $J\psi_t$ by the formula

$$\left(J\psi_t|_x\right)^2 = \det\left(\left(d\psi_t|_x\right)^* \circ \left(d\psi_t|_x\right)\right).$$

We will only be interested in the first and second derivative of $J\psi_t$ at $t = 0$ so we drop the $\mathcal{O}(t^3)$ terms to simplify notation. From $\psi_t = x + tX + \frac{t^2}{2}Z$ we get

$$d\psi_t|_x(\tau) = D_\tau \psi_t = \tau + tD_\tau X + \frac{t^2}{2}D_\tau Z.$$

Then $\left(d\psi_t|_x\right)^* \circ \left(d\psi_t|_x\right)$ has matrix

$$\begin{aligned}&\delta_{ij} + t\left(\langle \tau_i, D_{\tau_j}X\rangle + \langle \tau_j, D_{\tau_i}X\rangle\right)\\ &+t^2\left(\frac{1}{2}(\langle \tau_i, D_{\tau_j}Z\rangle + \langle \tau_j, D_{\tau_i}Z\rangle) + \langle D_{\tau_i}X, D_{\tau_j}X\rangle\right)\end{aligned}$$

Using the formula from Lemma 3 we calculate the determinant:

$$\begin{aligned}(J\psi_t)^2 &= 1 + 2t\cdot(\langle \tau_1, D_{\tau_1}X\rangle + \langle \tau_2, D_{\tau_2}X\rangle)\\ &\quad + t^2\Big(4\langle \tau_1, D_{\tau_1}X\rangle\langle \tau_2, D_{\tau_2}X\rangle - (\langle \tau_1, D_{\tau_2}X\rangle + \langle \tau_2, D_{\tau_1}X\rangle)^2\\ &\quad + (\langle \tau_1, D_{\tau_1}Z\rangle + \langle \tau_2, D_{\tau_2}X\rangle) + |D_{\tau_1}X|^2 + |D_{\tau_2}X|^2\Big)\\ &= 1 + 2t\cdot \mathrm{div}_N\, X + t^2\Big((\mathrm{div}_N\, X)^2 + \mathrm{div}_N\, Z\\ &\quad + \left|(D_{\tau_1}X)^\perp\right|^2 + \left|(D_{\tau_2}X)^\perp\right|^2 + 2\Lambda\Big)\end{aligned}$$

Where

$$(D_{\tau_i}X)^\perp = \langle \nu, D_{\tau_i}X\rangle = D_{\tau_i}X - \langle \tau_1, D_{\tau_i}X\rangle\tau_1 - \langle \tau_2, D_{\tau_i}X\rangle\tau_2$$

and

$$\Lambda = \langle \tau_1, D_{\tau_1}X\rangle\langle \tau_2, D_{\tau_2}X\rangle - \langle \tau_1, D_{\tau_2}X\rangle\langle \tau_2, D_{\tau_1}X\rangle.$$

The symbol Λ is introduced here for brevity of notation. For $X = \nu$ this becomes $\det \mathrm{II}$.

In the last step we used

$$\begin{aligned}(\operatorname{div}_N X)^2 &= (\langle \tau_1, D_{\tau_1}X\rangle + \langle \tau_2, D_{\tau_2}X\rangle)^2 \\ &= |\langle \tau_1, D_{\tau_1}X\rangle|^2 + 2\langle \tau_1, D_{\tau_1}X\rangle\langle \tau_2, D_{\tau_2}X\rangle + |\langle \tau_2, D_{\tau_2}X\rangle|^2\end{aligned}$$

and (recall that $\langle \tau_1, \tau_2\rangle = 0$)

$$\begin{aligned}\left|(D_{\tau_i}X)^\perp\right|^2 &= (D_{\tau_i}X - \langle \tau_1, D_{\tau_i}X\rangle\tau_1 - \langle \tau_2, D_{\tau_i}X\rangle\tau_2)^2 \\ &= |D_{\tau_i}X|^2 + |\langle \tau_1, D_{\tau_i}X\rangle|^2 + |\langle \tau_2, D_{\tau_i}X\rangle|^2 \\ &\quad - 2\langle \tau_1, D_{\tau_i}X\rangle\langle \tau_1, D_{\tau_i}X\rangle - 2\langle \tau_2, D_{\tau_i}X\rangle\langle \tau_2, D_{\tau_i}X\rangle \\ &= |D_{\tau_i}X|^2 - |\langle \tau_1, D_{\tau_i}X\rangle|^2 - |\langle \tau_2, D_{\tau_i}X\rangle|^2.\end{aligned}$$

So that together we obtain for $(\operatorname{div}_N X)^2 + \left|(D_{\tau_1}X)^\perp\right|^2 + \left|(D_{\tau_2}X)^\perp\right|^2$:

$$2\langle \tau_1, D_{\tau_1}X\rangle\langle \tau_2, D_{\tau_2}X\rangle + |D_{\tau_1}X|^2 + |D_{\tau_2}X|^2 - |\langle \tau_2, D_{\tau_1}X\rangle|^2 - |\langle \tau_1, D_{\tau_2}X\rangle|^2$$

The difference to the term in the formula for $(J\psi_t)^2$ above is

$$2\left(\langle \tau_1, D_{\tau_1}X\rangle\langle \tau_2, D_{\tau_2}X\rangle - \langle \tau_1, D_{\tau_2}X\rangle\langle \tau_2, D_{\tau_1}X\rangle\right) = 2\Lambda.$$

Finally we use

$$\left(1 + At + Bt^2\right)^2 = 1 + 2At + (A^2 + 2B)t^2 + \mathcal{O}(t^3)$$

to get the expression for $J\psi_t$:

$$J\psi_t = 1 + t\operatorname{div}_N X + \frac{t^2}{2}\left(\operatorname{div}_N Z + \left|(D_{\tau_1}X)^\perp\right|^2 + \left|(D_{\tau_2}X)^\perp\right|^2 + 2\Lambda\right).$$

4.2 First Variation

Now that we have an expression for the jacobian we can calculate the first variation of $J[N]$. The following can be found in Ilmanen [10].

$$\begin{aligned}
\frac{d}{dt}\Big|_{t=0}\int_{N_t} f(x) &= \frac{d}{dt}\Big|_{t=0}\int_N f(\psi_t(x))\cdot|J\psi_t(x)| \\
&= \int_N \frac{d}{dt}\Big|_{t=0}(f(\psi_t(x))\cdot|J\psi_t|) \\
&= \int_N \frac{d}{dt}f(\psi_t)\Big|_0\cdot 1 + f(x)\cdot\frac{d}{dt}J\psi_t\Big|_0 \\
&= \int_N \langle Df, X\rangle + f\,\mathrm{div}_N\, X \\
&= \int_N \langle Df, X\rangle + \mathrm{div}_N(fX) - \langle (Df)^\top, X\rangle \\
&= \int_N \langle (Df)^\perp, X\rangle - \langle fX, \vec{H}\rangle \\
&= \int_N \langle (Df)^\perp - f\cdot\vec{H}, X\rangle.
\end{aligned}$$

If a surface N satisfies the equation

$$(Df)^\perp - f\cdot\vec{H} = 0, \tag{4}$$

then the above integral is zero for every vector field X. Division by f and multiplication by ν yields

$$H - \frac{\langle Df, \nu\rangle}{f} = 0.$$

For

$$-\frac{Df}{f} = \frac{x}{2}$$

equation 4 becomes equivalent to (SS). So we solve for $f(x)$ and get

$$f(x) = C\cdot e^{-|x|^2/4}$$

with a constant C which can be choosen as $C = (4\pi)^{-1}$.

Note that in difference to the backward heat kernel of Huisken our $f(x)$ does not depend on time t. This is because the self-shrinker equation (SS) is specific for a certain time and setting $t = -1$ in Huisken's heat kernel leads to the same result.

Finally we get the functional

$$J[N] = \frac{1}{4\pi}\int_N e^{-|x|^2/4} d\mathcal{H}^2$$

and

Theorem 9 *If a surface N satisfies the self-shrinker equation (SS) it is stationary for the functional J, i. e. $\delta J[N] = 0$.*

4.3 Second Variation

In calculus the second derivative reveals information about the stability of an extremum. Let x_0 be an extremum of the real valued function $f(x)$. Then $f(x_0)$ is a maximum if $f''(x_0) < 0$ and a minimum if $f''(x_0) > 0$. For any algorithm that tries to minimize $f(x)$ a maximum is a highly unstable extremum whereas the minimum is stable. Being slightly off a maximum, the algorithm will diverge from it, whilst it always converges towards a minimum. For $f''(x_0) = 0$ we have a saddle point and then the stability depends on whether we are on the left or the right side of the extremum.

Roughly the same holds for a functional. The second variation reveals information about the stability of a stationary point. Unfortunately there is an infinity of possible stability directions so we do not expect to find a completely stable point at all – except for the singular point which has minimal area with respect to any metric. That's why we want to concentrate on a few well choosen stability directions.

Of course we first need to have an expression for the second variation. After finding an expression for general vector fields we will specialize on the case of normal vector fields $X = u\nu$ for some $u : N \to \mathbb{R}$. As mentioned earlier we are not interested in tangential motions anyway so that this special case is still general enough to handle all questions we impose in this paper.

Note that we are only interested in the stability of stationary points. In other words we do calculate the second variation for a surface for which the first variation is zero. This will permit some simplification.

$$\begin{aligned}
\frac{d^2}{dt^2}\Big|_{t=0}\int_{N_t} f &= \frac{d^2}{dt^2}\Big|_{t=0}\int_N f(\psi_t(x))\cdot|J\psi_t(x)| \\
&= \int_N \frac{d^2}{dt^2}\Big|_{t=0}(f(\psi_t(x))\cdot|J\psi_t|) \\
&= \int_N \frac{d^2}{dt^2}f(\psi_t)\cdot J\psi_t + 2\frac{d}{dt}f(\psi_t)\cdot\frac{d}{dt}J\psi_t + f(\psi_t)\cdot\frac{d^2}{dt^2}J\psi_t\Big|_0 \\
&= \int_N D^2f(X,X) + \langle Df, Z\rangle + 2\,\mathrm{div}_N X\langle Df, X\rangle + f\,\mathrm{div}_N Z \\
&\qquad + f\cdot\left(\left|(D_{\tau_1}X)^\perp\right|^2 + \left|(D_{\tau_2}X)^\perp\right|^2 + 2\Lambda\right) \\
&= \int_N D^2f(X,X) + 2\,\mathrm{div}_N X\langle Df, X\rangle \\
&\qquad + f\cdot\left(\left|(D_{\tau_1}X)^\perp\right|^2 + \left|(D_{\tau_2}X)^\perp\right|^2\right) \\
&\qquad + 2f\cdot(\langle\tau_1, D_{\tau_1}X\rangle\langle\tau_2, D_{\tau_2}X\rangle - \langle\tau_1, D_{\tau_2}X\rangle\langle\tau_2, D_{\tau_1}X\rangle)
\end{aligned}$$

In the last step we used the fact that $\langle Df, Z\rangle + f\,\mathrm{div}_N Z$ is zero because we are calculating the second variation at a point where the first variation is zero for any vector field X. Furthermore we do know Df from the calculations of the first variation and can also derive an expression for D^2f:

$$\begin{aligned}
Df &= -\frac{x}{2}f(x) \\
D^2f(X,X) &= \frac{1}{4}f(x)\cdot|\langle x, X\rangle|^2 - \frac{1}{2}f(x)\cdot|X|^2.
\end{aligned}$$

This leads to:

$$\begin{aligned}
\frac{d^2}{dt^2}\Big|_{t=0}\int_{N_t} f &= \int_N f(x)\Bigg(\frac{1}{4}|\langle x, X\rangle|^2 - \frac{1}{2}|X|^2 - \mathrm{div}_N X\langle x, X\rangle \\
&\qquad + \left|(D_{\tau_1}X)^\perp\right|^2 + \left|(D_{\tau_2}X)^\perp\right|^2 + 2\Lambda\Bigg)
\end{aligned}$$

Now set $X = u\nu$ for a function $u : N \to \mathbb{R}$. Because we do ignore tangential motions this is no additional constraint on possible motions of N. Also recall that because the first variation is zero, N is a self-shrinker and thus

$$\frac{\langle x, \nu\rangle}{2} + H = 0.$$

Furthermore $\Lambda = u^2\det(\mathrm{II})$ for $X = u\nu$ and therefore we can simplify the

second variation formula:

$$\begin{aligned}
\frac{d^2}{dt^2}\Big|_{t=0}\int_{N_t} f &= \int_N f(x)\Big(\frac{1}{4}|\langle x, u\nu\rangle|^2 - \frac{1}{2}|u\nu|^2 - \operatorname{div}_N(u\nu)\langle x, u\nu\rangle \\
&\qquad + \big|(D_{\tau_1}(u\nu))^\perp\big|^2 + \big|(D_{\tau_2}(u\nu))^\perp\big|^2 + 2u^2\det(\mathrm{II})\Big) \\
&= \int_N f(x)\left(u^2\left(\frac{\langle x,\nu\rangle}{2}\right)^2 - \frac{1}{2}u^2 - 2u^2\operatorname{div}_N\nu\cdot\frac{\langle x,\nu\rangle}{2}\right. \\
&\qquad \left. + |D_N u|^2 + 2u^2\det(D\nu^\top)\right) \\
&= \int_N f(x)\left(u^2H^2 - \frac{1}{2}u^2 - 2u^2H^2 + 2u^2\det\mathrm{II} + |D_N u|^2\right) \\
&= \int_N f(x)\left(-u^2H^2 - \frac{1}{2}u^2 + 2u^2\det\mathrm{II} + |D_N u|^2\right) \\
&= \int_N f(x)\left(u^2\left(2\det(\mathrm{II}) - H^2 - \frac{1}{2}\right) + |D_N u|^2\right) \\
&= \int_N f(x)\left(-u^2\left(|\,\mathrm{II}\,|^2 + \frac{1}{2}\right) + |D_N u|^2\right)
\end{aligned}$$

In the last step we used lemma 4 to replace $\det(\mathrm{II})$.

By lemma 1 we have

$$\begin{aligned}
\operatorname{div}_N(u\cdot D_N u) &= u\cdot\operatorname{div}_N(D_N u) + |D_N u|^2 \\
&= u\cdot\Delta_N u + |D_N u|^2.
\end{aligned}$$

Again by lemma 1 it is

$$f\cdot\operatorname{div}_N(u\cdot D_N u) = \operatorname{div}_N(f\cdot u\cdot D_N u) - \langle (Df)^\top, uD_N u\rangle.$$

Putting this together yields:

$$\begin{aligned}
\int_N f\cdot|D_N u|^2 &= \int_N f\cdot\operatorname{div}_N(u\cdot D_N u) - f\cdot u\cdot\Delta_N u \\
&= \int_N \operatorname{div}_N(f\cdot u\cdot D_N u) - u\langle (Df)^\top, D_N u\rangle - f\cdot u\cdot\Delta_N u \\
&= \int_N -u\langle Df, D_N u\rangle - f\cdot u\cdot\Delta_N u \\
&= \int_N -\frac{1}{2}u\cdot f\langle -x, D_N u\rangle - f\cdot u\cdot\Delta_N u.
\end{aligned}$$

And finally we get for the second variation:

$$\begin{aligned}\frac{d^2}{dt^2}\Big|_{t=0}\int_{N_t} f &= \int_N f(x)\left(-u^2\left(|\,\mathrm{II}\,|^2+\frac{1}{2}\right)-u\cdot\Delta_N u+\frac{1}{2}u\langle x, D_N u\rangle\right)\\ &= \int_N -f(x)\cdot u\cdot\left(|\,\mathrm{II}\,|^2 u+\frac{1}{2}u-\frac{1}{2}\langle x, D_N u\rangle+\Delta_N u\right)\\ &= \int_N -f(x)\cdot u\cdot L(u)\end{aligned}$$

where

$$L(u)=\Delta_N u-\frac{1}{2}\langle x, D_N u\rangle+|\,\mathrm{II}\,|^2 u+\frac{1}{2}u.$$

4.4 The linear operator $L(u)$

As mentioned above there are an infinite number of possible functions $u : N \to \mathbb{R}$ and associated stability directions. In addition the functions u depend on the surface N and therefore it is very difficult to get general results concerning stability. However if u is an eigenfunction of $L(u)$ with eigenvalue λ it is easy to derive general results.

Assume that λ is the eigenvalue for $L(u)$ associated with u_λ. Then we get:

$$\frac{d^2}{dt^2}\Big|_{t=0}\int_{N_t} f = -\lambda\int_N f(x)u_\lambda^2.$$

The integral on the right side is always positive because $f(x)$ and u_λ^2 are positive everywhere. Therefore the stability depends solely on the eigenvalue λ. For positive λ the right side becomes negative. So the stationary point is a maximum. For negative λ the stationary point is a minimum and therefore stable under u. Thus we call a surface N *stable* if $L(u)$ has no positive eigenvalues.

We expect some important vector fields X to induce eigenfunctions u. In particular the rotation $X = Lx$ will induce an eigenfunction with eigenvalue $\lambda = 0$. This is because the functional $J[N]$ is rotationally symmetric and rotating any surface with fixed origin does not change the functional $J[N]$.

On the other hand there are indications that the eigenvalues induced by a homothety $X = \mu x$ or a translation $X = a$ for a fixed $a \in \mathbb{R}^3$ are positive. We will present the numerical indications in the next chapter.

A surface N that is stable except perhaps for a homothety or a translation does not change shape. Accordingly we call the surface N *geometrically stable* if the

only possible positive eigenvalues of $L(u)$ are the ones coming from a homothety or a translation.

Unfortunately it was not possible to develop this theory further in time and so it has to remain for future investigation.

5 Numerics

Most of the self-shrinkers known today are only known in form of numerical approximations. Actually the existence of these self-shrinkers is not proved but only indicated by various computations. We will present here a further algorithm to find self-shrinkers numerically. Beside that we will also introduce some of the previously found self-shrinkers.

5.1 Gaussian space

The starting point for our algorithm lies in the observation that self-shrinkers are stationary for the functional

$$J[N] = \frac{1}{4\pi} \int_N e^{-|x|^2/4} d\mathcal{H}^2. \tag{5}$$

Thus the search for self-shrinkers is equivalent to the search for stationary surfaces for $J[N]$.

We can interpret the functional $J[N]$ as the area functional of a space endowed with the "Gaussian" metric

$$f(x) = \frac{1}{4\pi} e^{-|x|^2/4}. \tag{6}$$

Invoking the mean curvature flow of this modified space will minimize the functional $J[N]$ for the very same surface in euclidean space. Hopefully this will converge to a stationary point.

According to the well known first variation formula

$$\delta A[N] = -\int_N \langle X, \vec{H} \rangle d\mathcal{H}^2$$

a surface decreases its area under mean curvature flow ($X = \vec{H}$) unless it is stationary for the area functional. Therefore a surface converges to a stationary point or evolves into a singularity with zero area. This convergence lies at the heart of our algorithm.

We will denote the space $\mathbb{R}^3$ endowed with the metric $f(x)$ from (6) by $\mathbb{G}^3$ and call it *Gaussian space*. Note that the area functional $A[N]$ in Gaussian space corresponds to the functional $J[N]$ in euclidean space. For clarity we will mostly refer to the area of a surface inside $\mathbb{G}^3$ as J.

5.2 Stability

Unfortunately the metric $f(x)$ in (6) introduces new instabilites. For instance euclidean space $\mathbb{R}^3$ is invariant under translation whereas $\mathbb{G}^3$ is not, as the following example shows.

Example: Translation of a plane Let P be a plane parallel to the xy-plane. Then z is the distance of P from the origin. We calculate the functional $J[N]$ (which corresponds to the area of P inside $\mathbb{G}^3$) in dependance of z:

$$\begin{aligned} J[P] &= \frac{1}{4\pi}\int_P e^{-|\vec{x}|^2/4} d\mathcal{H}^2 \\ &= \frac{1}{4\pi} e^{-z^2/4} \int_0^\infty \int_0^\infty e^{-(x^2+y^2)/4} dxdy \\ &= e^{-z^2/4} \end{aligned}$$

Note that we exceptionally wrote $\vec{x} = (x, y, z)$. Obviously a plane can diminuish

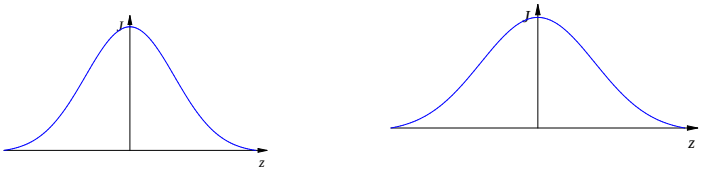

Figure 6: *The area of the plane with respect to the distance from the origin (left) and the area of a sphere with constant radius, moved away from the origin (right). Both in Gaussian space.*

its area by moving away from the origin. As long as the surface moves by mean curvature the plane will not move because $H \equiv 0$. But the slightest perturbation will cause the plane to become unstable and start moving. In particular this instability plays a role for any surface with $H \not\equiv 0$.

Homothetic instability In contrast to euclidean space the scale of the surface does also play a crucial role. This is hardly surprising because the stationary surfaces are the self-shrinkers at time $t = -1$ and as mentioned before they need to have a very specific size.

Example: Homothetic expansion of a sphere Clearly the area of the sphere depends on the radius – even in Gaussian space. But in contrast to euclidean

space there is a second stationary radius besides $r = 0$ (which is the singularity that always exists as stationary point). For the radius r we get the following Gaussian area for the Sphere:

$$\begin{aligned} J[S^2] &= \frac{1}{4\pi}\int_{S^2} e^{-|x|^2/4} d\mathcal{H}^2 \\ &= \frac{1}{4\pi} e^{-r^2/4} \int_{S^2} d\mathcal{H}^2 \\ &= \frac{1}{4\pi} e^{-r^2/4} \cdot 4\pi r^2 \\ &= r^2 e^{-r^2/4}. \end{aligned}$$

Figure 7 shows the graph for $J[S^2]$ in dependence of the radius r. The mentioned stationary point which is a maximum is clearly seen. To find the precise value we differentiate $J[S^2]$ with respect to r:

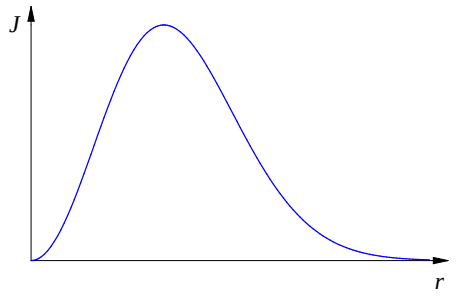

Figure 7: *The area of a sphere with respect to the radius in Gaussian space.*

$$\frac{d}{dr} J[S^2] = \left(2r - \frac{1}{2}r^3\right) e^{-r^2/4} = -\frac{r}{2}(r^2 - 4)e^{-r^2/4}.$$

Therefore the maximum seen in figure 7 is located at $r = 2$. It is the only extremum besides $r = 0$ and $r = \infty$. This corresponds exactly to the result we derived earlier stating that the self-shrinking sphere needs to have a radius of $r = 2$ at time $t = -1$.

The example of the homothetically expanded sphere shows a stability problem occuring for homotheties. If a sphere is slightly off the stationary radius $r = 2$ it will never converge to this stationary point. Rather it will shrink to a point or expand to infinity, where the Gaussian area vanishes due to the fast decay of the Gaussian metric.

For other surfaces such as the cylinder this stability turns out to be even worse. A cylinder that is slightly off the stationary radius will not only shrink to a point

or expand to infinity but also change shape rapidly. We will go into more details later.

Controlling the instabilities Among the three geometrical instabilities – rotation, translation and homothety – the rotation is of no interest to us. It has no effect on J and we therefore ignore it.

The instability of translation can easily be controlled by symmetry. This is because on a symmetric surface translatory forces compensate each other. The surfaces we investigate are all highly symmetric and so we can neglect this instability here. But note that a slight perturbation could cause the surface to become unstable and start moving. Translatory instabilities also become an issue when dealing with surfaces that are not symmetric with respect to the origin.

The final instability of homotheties must be controlled manually. This control is one of the center pieces of our algorithm. Roughly speaking the algorithm pushes the surface back to a size near the extremum whenever needed. Unfortunately we can barely hope to hit the stationary point precisely enough to keep the surface from shrinking or expanding. The details will be given below.

5.3 Surfaces of rotation

When a surface N is obtained by rotating a curve γ around the z-axis it is possible to formulate a condition for the curve γ that is equivalent to N being a self-shrinker. By doing so we can reduce a three-dimensional problem to a two-dimensional problem.

Angenent used this idea to prove that there is a self-shrinking torus. He showed that there is a closed curve γ in the plane that creates a self-shrinking torus by rotation.

Let $\gamma = (u(t), v(t))$ be a curve inside the plane with $u(t) \geq 0$ (to avoid confusion we denote the two axes with u and v instead of x and z). Then we get a surface by rotating γ around the z axis, obtaining

$$F(\varphi, t) = \begin{pmatrix} \cos(\varphi)u(t) \\ \sin(\varphi)u(t) \\ v(t) \end{pmatrix}.$$

Recall that the metric is calculated by $g_{ij} = \langle \partial_i F, \partial_j F \rangle$. We have:

$$\frac{\partial F}{\partial \varphi} = \begin{pmatrix} -\sin(\varphi)u(t) \\ \cos(\varphi)u(t) \\ 0 \end{pmatrix}, \qquad \frac{\partial F}{\partial t} = \begin{pmatrix} \cos(\varphi)u'(t) \\ \sin(\varphi)u'(t) \\ v'(t) \end{pmatrix}.$$

This gives the metric

$$g = \begin{bmatrix} u^2(t) & 0 \\ 0 & (u'(t))^2 + (v'(t))^2 \end{bmatrix}.$$

We can now compute the functional $J[N]$:

$$\begin{aligned} J[N] &= \int_N f(\vec{x}) d\mathcal{H}^2 \\ &= \int_N f(\vec{x}) \sqrt{\det g}\, d\varphi\, dt \\ &= \int_\gamma \int_0^{2\pi} f(\vec{x}) u(t) \sqrt{(u')^2 + (v')^2}\, d\varphi\, dt \\ &= 2\pi \int_\gamma f(\vec{x}) u(t) d\mathcal{H}^1. \end{aligned}$$

Using the Gaussian functional $f(x) = \frac{1}{4\pi} e^{-|\vec{x}|^2/4}$ and $|\vec{x}|^2 = u^2 + v^2$ we get

$$J[N] = \frac{1}{2} \int_\gamma u\, e^{-|u^2+v^2|/4} d\mathcal{H}^1.$$

Therefore we get the following theorem:

Theorem 10 *A surface N obtained by rotating the curve γ is a solution to (SS) iff $\gamma : t \mapsto (x, y)$ is stationary for the functional*

$$K[\gamma] = \int_\gamma u\, e^{-|x^2+y^2|/4} d\mathcal{H}^1.$$

Again we can interpret $K[\gamma]$ as the length functional of a two-dimensional space endowed with the metric $g(x, y) = x \exp(-|x^2+y^2|/4)$. For convenience we will refer to this space as K-space.

Sphere and cylinder Of course the sphere and the cylinder are rotationally symmetric surfaces. So there are curves γ_S and γ_C respectively that create the sphere or the cylinder when rotated. We will not prove here that these curves γ_S and γ_C are geodesics for the K-space defined above. However we will show

that the radius for the sphere obtained through this method is the same as the radius we obtained in previous chapters.

For the sphere we have for $\alpha \in [-\frac{\pi}{2}, \frac{\pi}{2}]$ and the radius R:

$$\gamma(t) = \begin{pmatrix} R\cos(\alpha) \\ R\sin(\alpha) \end{pmatrix}.$$

For K we get:

$$\begin{aligned} K[\gamma] &= \frac{1}{2}\int_{-\frac{\pi}{2}}^{\frac{\pi}{2}} R\cos(\alpha)e^{-R^2/4} \cdot Rd\alpha \\ &= \frac{1}{2}R^2e^{-R^2/4}\int_{-\frac{\pi}{2}}^{\frac{\pi}{2}} \cos(\alpha)d\alpha \\ &= R^2e^{-R^2/4}. \end{aligned}$$

To obtain a maximum for R we differentiate with respect to R.

$$\frac{d1}{dR}K[\gamma] = \left(2R - \frac{1}{2}R^2\right)e^{-R^2/4} = -\frac{1}{2}R(R^2-4)e^{-R^2/4}.$$

This is the same expression as we obtained earlier and again the radius for the sphere is $R = 2$.

Angenent's doughnut The advantage of this reduction is that it suffices to find a geodesic in the plane endowed with the metric $x\exp(-|x^2+y^2|/4)$. This can be done using theory of differential equations. Angenent proved this way that there is a geodesic γ inside the plane with the above metric that is closed and symmetric. Therefore there exists a self-shrinking torus.

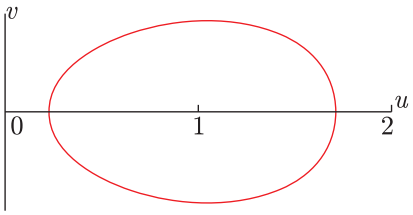

Figure 8: *The geodesic that creates Angenent's doughnut when rotated around the v-axis. This picture is taken from Chopp [4].*

5.4 The algorithm

The algorithm is comprised of two steps. In a first step the surface is evolved under mean curvature flow or a similar flow in order to locally minimize the Gaussian area J. In a second step the surface is renormalized by homothety to compensate for the homothetic instability.

First step: evolving The first step is responsible for the local minimization of the Gaussian area J. This can be done by mean curvature flow. But since we are interested in finding a stationary point for J we can invoke basically any flow that locally minimizes J.

Figure 9: *The force at each vertex results from the attempt to minimize the adjacent triangles (faces). The resulting force of a vertex can then be used to mimic mean curvature flow.*

The surface evolver of Brakke represents the surfaces by a triangulation. The basic assumption for the evolution is that each triangle attempts to minimize its area, resulting in a force vector on each of its three vertices (see figure 9). The evolver then calculates the resulting force vector for each vertex. Finally it determines an optimal scale factor σ such that the surface moved by the vertex force vectors times σ minimizes the area.

Second step: renormalization The surface evolver has no inbuilt function for renormalization as we invoke it in the second step of our algorithm. Recall that the aim of this step is to control the homothetic instability by rescaling a surface such that the Gaussian area J becomes stationary under homothety.

Although we do not provide a proof for it, the algorithm assumes that the Gaussian area has to be maximizied in order to find the stationary point. If this was not the case the surface would be stable under homothety anyway and we would not need to invoke this second step. Thus the purpose of the subroutines

provided here is to find the maximum of a function $f(\lambda)$ which happens to be the Gaussian metric J in our case.

For any surface N a homothetic expansion by the factor λ results in a surface λN for which we can calculate the Gaussian area:

$$\begin{aligned} J[\lambda N] &= \int_{\lambda N} f(x) d\mathcal{H}^2 \\ &= \int_N f(\lambda x)\lambda^2 d\mathcal{H}^2 \\ &= \int_N \frac{1}{4\pi} e^{-\lambda^2|x|^2/4}\lambda^2 d\mathcal{H}^2. \end{aligned}$$

Thus instead of performing real expansion we can also modify the metric of the Gaussian space in order to obtain $J[\lambda N]$. The metric used in our datafiles therefore contains an additional parameter λ which is set to $\lambda = 1$ during most of the time. By changing λ we then can simulate an expansion. Inside the program this parameter λ is called `mpar` – short for **m**etric **par**ameter.

Finding the maximum Let $f(x)$ be a real valued function and assume that $f(x)$ has exactly one maximum for $0 < x < \infty$. We assume further that the maximum is somewhere "near" the point $x_0 = 1$. Then we have the following algorithm for the initial value $x_0 = 1$ and the initial stepwidth Δ.

[1] Calculate the values $y_n^- = f(x_n - \Delta)$, $y_n = f(x_n)$ and $y_n^+ = f(x_n + \Delta)$.

[2] Determine the largest value of y_n^-, y_n, y_n^+. If y_n^- is the maximum then set $x_{n+1} = x_n - \Delta$ and go back to [1]. If y_n^+ is the maximum then set $x_{n+1} = x_n + \Delta$ and go back to [1].

[3] If y_n^- and y_n^+ are both smaller than y_n then refine the stepwidth $\Delta' = \frac{1}{2}\Delta$ and try again with step [1].

The exact value $x_{\max}$ for which $f(x_{\max})$ is a maximum might be an irrational number or another number that exceeds the accuracy of the used floating point numbers. In that case the algorithm might run for a very long time trying to find an exact value by refining the stepwidth. That's why the algorithm is limited to a maximum number of iterations $N_{\max}$. This in turn also limits the possible accuracy of the result to $2^{-N_{\max}}\Delta$.

When a possible maximum value $x_{\max}$ is found $f(x)$ is transformed to a new function $\tilde{f}(x)$ such that the maximum value is mapped to 1: $f(x_{\max}) = \tilde{f}(1)$.

Applying the maximum-algorithm For any surface the maximum-algorithm as depicted above is applied to the Gaussian area $J[N]$, that is $f(\lambda) = J[\lambda N]$. As mentioned earlier the $J[\lambda N]$'s are evaluated by changing the metric. After the maximum-algorithm has found a maximizing λ (which could be 1), the surface is actually expanded or shrinked by the factor λ.

As the surface converges to a stationary one, the homothety factor λ converges to 1. To keep up the desired accuracy the initial stepwidth Δ will be choosen smaller with time, confining the maximum-algorithm to a smaller range but allowing it to find the factors λ with more accuracy.

Source code Below we present the actual evolver source code used for the algorithm. The reader who is familiar with the evolver might find it handy. The algorithm works fine with different surfaces but the actual expansion procedure has to be modified to suit the needs of the surfaces (e. g. respecting constraints).

Note that the actual implementation of the algorithm given below differs slightly from the algorithm described above. The two cases of expansion ($\lambda > 1$) and shrinking ($\lambda < 1$) are completely separated. This is due to an earlier draft that was used for the actual computations. However the basic idea remains the same.

```
/*
 *  METRIC
 */
conformal_metric
1/(4*pi)*e^(-(x^2+y^2+z^2)*mpar^2/4)*mpar^2

/*
 *  The surface-data and constraints would appear here.
 */

/*
 *  READ-SECTION
 */
read

/*
 *  The following parameters are used inside the algorithm.
 */
par := 1;
max_find_steps := 50;
metric_delta := 1/32;

/*
 *  "ex" is a command to expand or shrink the surface
 *  homothetically. May be changed in order to respect
```

```
 *  the constraints.
 */
ex := {set vertex x x*par;
       set vertex y y*par;
       set vertex z z*par}

/*
 *  "find_expand" expands the surface until the expansion would
 *  decrease the area. Thus we can find a maximum.
 */
find_expand := {
  TA_1 := total_area;
  mpar_orig := mpar;
  n_delta := metric_delta;
  for (var_I := 1; var_I < max_find_steps; var_I += 1)
    {
      mpar += n_delta;
      recalc;
      TA_2 := total_area;
      if (TA_2 <= TA_1)
        then {mpar -= n_delta; n_delta := n_delta / 2}
        else {TA_1 := TA_2};
    };
  par := mpar;
  mpar := mpar_orig;
}

/*
 *  "find_shrink" shrinks the surface until the shrinked surface
 *  would decrease the area.
 */
find_shrink := {
  TA_1 := total_area;
  mpar_orig := mpar;
  n_delta := metric_delta;
  for (var_I := 1; var_I < max_find_steps; var_I += 1)
    {
      if (n_delta >= mpar) then {n_delta := mpar * 0.45};
      mpar -= n_delta;
      recalc;
      TA_2 := total_area;
      if (TA_2 <= TA_1)
        then {mpar += n_delta; n_delta := n_delta / 2}
        else {TA_1 := TA_2};
    };
  par := mpar;
  mpar := mpar_orig;
}

/*
 *  "find_max" tests whether the surface should be expanded or
 *  shrinked and calls then "find_expand" or "find_shrink"
 *  respectively.
 */
find_max := {
  TA_1 := total_area;
  mpar_orig := mpar;
  mpar -= metric_delta;
```

```
  recalc;
  TA_2 := total_area;
  mpar :=  mpar_orig;
  recalc;
  if (TA_2 > TA_1)
    then find_shrink
    else find_expand;
  if not (par = 1) then ex;
}

/*
 *  The "gg"-command evolves two steps under MCF and then applies
 *  the "find_max"-algorithm. "next" refines the stepwidth for the
 *  "find_max"-algorithm.
 */
gg := {g 2; find_max}
next := {metric_delta /= 4};
```

5.5 Self-shrinkers

In this chapter we finally discuss some possible self-shrinkers. We will start with the most simple ones and then proceed to more complicated surfaces. Many more can be found in Chopp [4] or Ilmanen [10].

Sphere Apart from the plane the sphere is definitely the most simple self-shrinker. Nevertheless the sphere is homothetically unstable as mentioned before. It provides therefore a good testing ground for the algorithm.

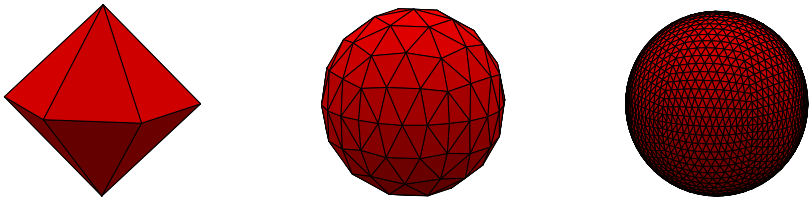

Figure 10: *We start off with a polyhedron that is topologically equivalent to the sphere and then evolve it in order to find the sphere as a stationary surface.*

Starting with a polyhedron as seen in figure 10 the surface converges indeed to a sphere – as far as a triangulated surface can represent a sphere at all. From the calculations made before the expected radius of this sphere is $R = 2$. Because of the triangulation this result will hardly be achieved. Comparing the distances of all vertices from the origin one finds that $R \in [1.9986; 2.0047]$ which is off the exact result less than 0.5%.

Cylinder The second surface to test the algorithm is the cylinder. Although the cylinder is a very simple surface with many similarities to the sphere, it turns out that evolving the cylinder is much harder than evolving the sphere.

For one thing the cylinder is not a compact surface but extends to infinity. This of course cannot be done with a computer. We need to chop the infinite cylinder and work with a relatively small segment of it.

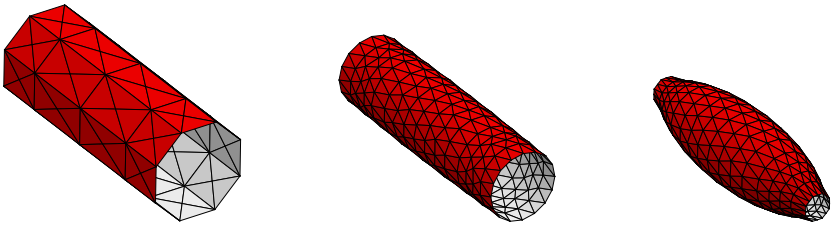

Figure 11: *When evolving the cylinder, it comes up with an unexpected instability and eventually converges to the sphere.*

To take the infinite size of the cylinder into account we impose constraints on the two borders. The nature of these constraints influences the behaviour of the cylinder. As the computer tries to minimize area, the facets adjacent to the border tend to be perpendicular to the imposed constraint as seen in figure 12. This is because the shortest distance between a surface and a point is a straight line perpendicular to the surface.

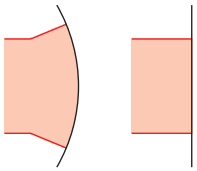

Figure 12: *The facets of the surface (red) that touch the constraint (black) tend to be perpendicular to the constraint. This can cause perturbations.*

In our computations we found it nearly impossible to create a stable cylinder. This might have several reasons. There might be a further instability direction we did not yet take into account. In particular we could not impose a translatory symmetry that would force the cylinder to act more homogeneously.

Furthermore with the chopping of the cylinder to a finite length we loose an important information. beyond the chopping border the cylinder could have caps

instead of reaching to infinity. In that case the surface is convex and therefore has to converge to a sphere, according to theorem 5.

Whilst it might be possible to modify the algorithm to control an additional instability in a similar way as we did for the homothetic instability, the second consideration indicates that we are actually dealing with a completely new problem. Then the chopping of the cylinder is not as harmless as expected but causes a substantial change.

An attempt to increase the length of the cylinder section did not work out. Because of the Gaussian metric the computation of the forces far away from the origin has significant rounding errors. In fact the endings of the cylinder did not move at all but stayed in their polygonial initial shape.

Desingularized surfaces The simplest self-shrinkers are the plane, the sphere and the cylinder. In order to find new self-shrinkers it is therefore natural trying to combine any two of these three to build a new surface.

Unfortunately the union of two simple self-shrinkers creates singularities just as the union of two planes would along the intersection line. So to get a regular smoothly embedded surface the singularities are removed by tiny holes along the intersection lines, inspired by the Scherk tower. The so obtained surface is expected to converge then to a self-shrinker very similar to the starting surface.

Xuan Hien Nguyen describes the process in more detail and provides a partial proof that the union of the plane and a cylinder indeed can be slightly altered to become a self-shrinker. However we will not go into details of the theoretical results here but concentrate on numerical results. See [12] for details.

Union of sphere and plane The union of a sphere and a plane has already been investigated by Ilmanen (see [10]). In particular he has numerically found two self-shrinking surfaces. The first one with three holes on either side (top and bottom) does not particularly resemble the union of a sphere and a plane. But the second one with nine holes on either side looks strongly like the union of a sphere and a cylinder.

Another surface of this class was found by Chopp (see [4]). It is a punctured saddle, as shown in figure 15. Note that there is a symmetry that maps the

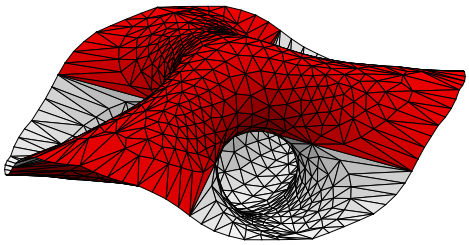

Figure 13: *The triply punctured surface found by T. Ilmanen. This picture was recreated using our algorithm.*

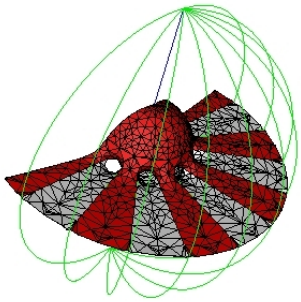

Figure 14: *The nonuply punctured surface found by T. Ilmanen. The picture can be found on Ilmanen's homepage.*

handle onto the hole. What we see as handle here becomes a hole when viewed from below whereas our hole becomes the handle.

Union of cylinder and plane The union of the plane and the cylinder suffers from the same instability problem as does the cylinder. Our initial surfaces converge to the surfaces found by Ilmanen and Chopp (see preceding section). The peak seen in the final pictures is due to the constraints we imposed on the upper and lower borders. At these points the surface would naturally pinch off and change topology.

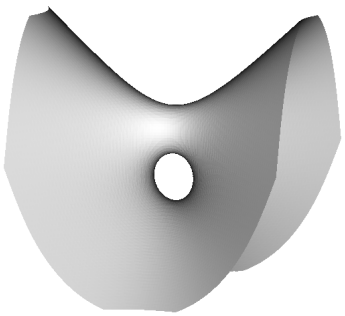

Figure 15: *The punctured saddle found by D. Chopp.*

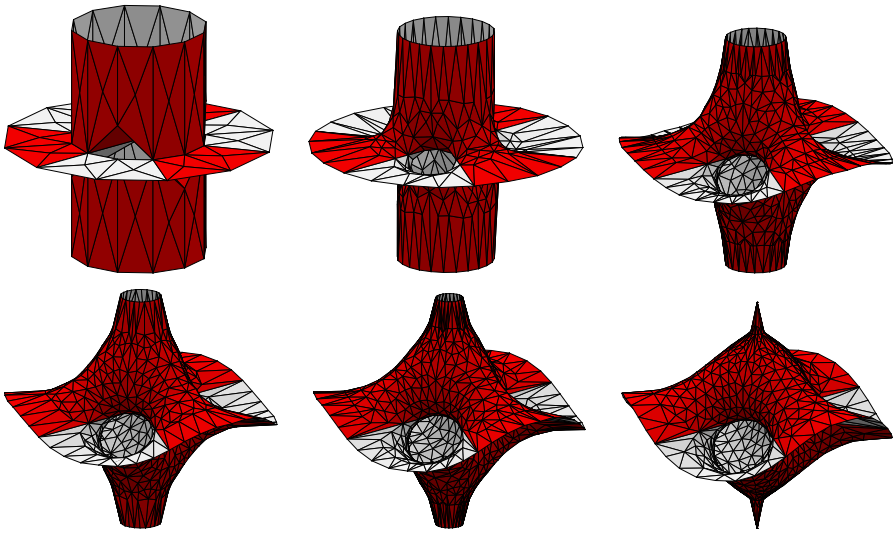

Figure 16: *Evolving the cylinder union a plane with 3 holes.*

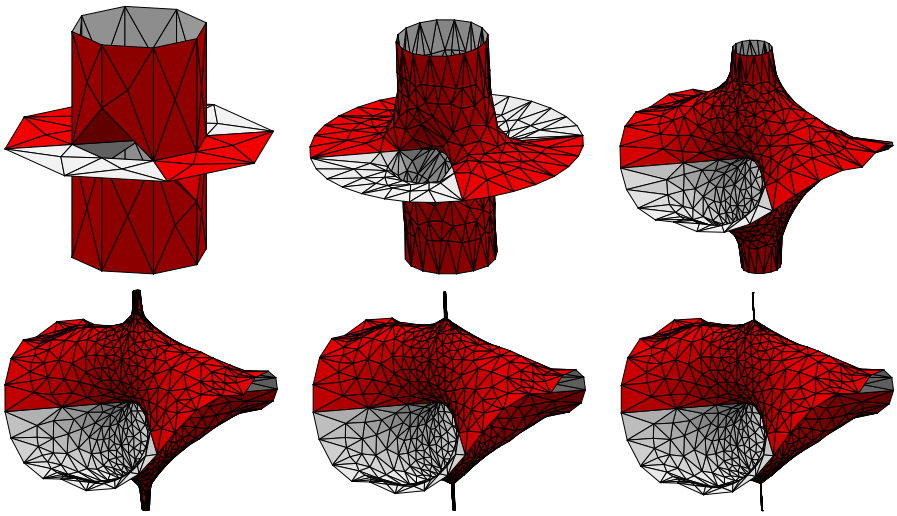

Figure 17: *Evolving the cylinder union a plane with 2 holes.*

References

[1] Sigurd B. Angenent: Shrinking doughnuts. In *Nonlinear diffusion equations and their equilibrium states, 3 (Gregynog, 1989)*, Volume 7 of *Progress in Nonlinear Differential Equations and Their Applications*, Birkhäuser, Boston 1992.

[2] Sigurd B. Angenent, David L. Chopp, Tom Ilmanen: A computed example of nonuniqueness of mean curvature flow in $\mathbb{R}^3$. In *Comm. Partial Differential Equations*, 20 (1995).

[3] Kenneth A. Brakke: Surface Evolver Manual. `http://www.susqu.edu/evolver`.

[4] David L. Chopp: Computation of Self-Similar Solutions for Mean Curvature Flow. Experimental Mathematics, 3 (1994), p. 1-15.

[5] Klaus Ecker: Regularity Theory for Mean Curvature Flow. Volume 57 of *Progress in Nonlinear Differential Equations and Their Applications*, Birkhäuser, Boston 2004.

[6] Jost-Hinrich Eschenburg, Jürgen Jost: Differentialgeometrie und Minimalflächen. Springer, Berlin 2007.

[7] Jörg Hättenschweiler: Mean Curvature Flow of Networks with Triple Junctions in the Plane. Preprint 2007.

[8] Gerhard Huisken: Asymptotic behaviour for singularities of the mean curvature flow. In *Journal Differential Geometry* 31 (1990), p. 285-299.

[9] Gerhard Huisken: Flow by mean curvature of convex surfaces into spheres. In *Journal Differential Geometry* 20 (1984), p. 237-266.

[10] Tom Ilmanen: Lectures on Mean Curvature Flow and Related Equations. Preprint 1998.

[11] Frank Morgan: Riemannian Geometry – A Beginner's Guide. A K Peters, Natick 1998.

[12] Xuan Hien Nguyen: Construction of complete embedded self-similar surfaces under mean curvature flow. Part I and II, Preprint.

[13] Leon Simon: Lectures on Geometric Measure Theory. Proc. Centre Math. Anal. Austral. Nat. Univ., 3 (1983).